Hamiltonian replica exchange molecular dynamics using soft-core interactions

Hritz, J.; Oostenbrink, C.

published in
Journal of Chemical Physics
2008

DOI (link to publisher)
10.1063/1.2888998

document version
Publisher's PDF, also known as Version of record

Hamiltonian replica exchange molecular dynamics using soft-core interactions

Jozef Hritz and Chris Oostenbrink[a)]
Leiden Amsterdam Center for Drug Research (LACDR), Division of Molecular Toxicology, Vrije Universiteit, Amsterdam NL-1081 HV, The Netherlands

(Received 19 December 2007; accepted 5 February 2008; published online 14 April 2008)

To overcome the problem of insufficient conformational sampling within biomolecular simulations, we have developed a novel Hamiltonian replica exchange molecular dynamics (H-REMD) scheme that uses soft-core interactions between those parts of the system that contribute most to high energy barriers. The advantage of this approach over other H-REMD schemes is the possibility to use a relatively small number of replicas with locally larger differences between the individual Hamiltonians. Because soft-core potentials are almost the same as regular ones at longer distances, most of the interactions between atoms of perturbed parts will only be slightly changed. Rather, the strong repulsion between atoms that are close in space, which in many cases results in high energy barriers, is weakened within higher replicas of our proposed scheme. In addition to the soft-core interactions, we proposed to include multiple replicas using the same Hamiltonian/level of softness. We have tested the new protocol on the GTP and 8-Br-GTP molecules, which are known to have high energy barriers between the *anti* and *syn* conformation of the base with respect to the sugar moiety. During two 25 ns MD simulations of both systems the transition from the more stable to the less stable (but still experimentally observed) conformation is not seen at all. Also temperature REMD over 50 replicas for 1 ns did not show any transition at room temperature. On the other hand, more than 20 of such transitions are observed in H-REMD using six replicas (at three different Hamiltonians) during 6.8 ns per replica for GTP and 12 replicas (at six different Hamiltonians) during 8.7 ns per replica for 8-Br-GTP. The large increase in sampling efficiency was obtained from an optimized H-REMD scheme involving soft-core potentials, with multiple simulations using the same level of softness. The optimization of the scheme was performed by fast mimicking [J. Hritz and C. Oostenbrink, J. Chem. Phys. **127**, 204104 (2007)]. © *2008 American Institute of Physics*. [DOI: 10.1063/1.2888998]

I. INTRODUCTION

The energy landscape for biomolecules in explicit solvent exhibits many local free energy minima.[1] While many minima are readily sampled in a molecular dynamics (MD) simulation, some are separated by high free energy barriers.[2] A molecule can be trapped in local energy minimum conformations for times comparable to or longer than typical simulation times that are reachable by conventional MD. In these cases, regular MD simulations will not lead to a complete conformational sampling of the studied system.[3]

One possible solution is the application of temperature replica exchange MD (T-REMD), in which several parallel simulations are performed at different temperatures. At regular intervals switches of the temperature between simulations are attempted, allowing high temperature simulations to cool down and low temperature simulations to heat up. A gain in efficiency should be obtained if the free energy barriers can be easily crossed in high temperature simulations.[4] T-REMD, however, suffers from the fact that the number of replicas needed to cover the necessary temperature range is proportional to the square root of the number of degrees of freedom of the system. This means that T-REMD simulations of biomolecules in explicit solvent can be computationally very demanding. The requirement of a large number of replicas in T-REMD can be overcome by applying Hamiltonian REMD (H-REMD),[5,6] where not the temperature but the Hamiltonian is varied over the replicas, through a perturbation of the original Hamiltonian. Note that T-REMD is a special case of H-REMD in which all the terms in the Hamiltonian are multiplied by the same scaling factor.

Hamiltonians can be perturbed in different ways. Useful approaches are those, in which the free energy landscape of the higher replicas allows for faster conformational conversions compared to the unperturbed Hamiltonian at the lowest replica.

We choose to perturb the Hamiltonian by describing selected interactions with a soft-core potential[7] and vary the level of softness over the replicas through a softness parameter λ. This approach allows for a diminishing of free energy barriers at higher replicas with higher levels of softness. The advantage of our approach is that we can specifically use soft-core interactions for those biomolecular parts that are of interest, e.g., parts contributing the most to the free energy barriers between different conformations. In this study we have also applied the novel concept of a degenerate highest level of softness λ_{max}. This involves multiple (n) replicas at

[a)]Electronic mail: c.oostenbrink@few.vu.nl.

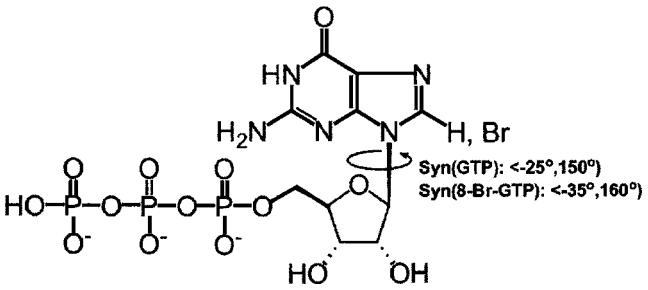

FIG. 1. Structure of GTP and 8-Br-GTP in *syn* conformation. Conformational transitions between the *syn* and *anti* states occur by rotation around the glycosidic bond (indicated). The glycosidic dihedral angle (ϕ) is defined over atoms: C4-N9-C1′-O4′.

λ_{max}, allowing the system to spend more time at this λ-value so that alternative conformations can be reached in shorter overall simulation time. This is reminiscent of the J-walking method[8] or finite reservoir simulations,[9,10] where a reservoir of structures is pregenerated at the highest temperature or Hamiltonian (T_{max}/λ_{max}) and then "coupled" to REMD to get correct ensembles at lower values of T or λ. However, the concept of a degenerate T_{max}/λ_{max} is an integral part of REMD requiring no precalculation. It allows for the most efficient balance between conformational transitions at T_{max}/λ_{max} and replica exchanges toward T_0/λ_0. Refinement of the optimal n and the optimal selection of λ-values by fast REMD mimicking is described in our previous paper.[11]

We have tested the H-REMD scheme using soft-core interactions on two biologically relevant systems: GTP and 8-Br-GTP (Fig. 1). These systems can adopt two stable conformations by rotation around the glycosidic bond: *Anti* and *syn*. The boundaries of these conformations are not exactly the same for GTP and 8-Br-GTP. Based on the dihedral angle distributions shown in the Results section, we consider GTP to be in a *syn* conformation if the dihedral angle around the glycosidic bond is within the interval $\langle -25°, 150° \rangle$. For 8-Br-GTP we use the interval $\langle -35°, 160° \rangle$ to define the *syn* state. NMR studies indicate that the dominant conformation for GTP is *anti*, while it is *syn* for 8-Br-GTP.[12] Both GTP and 8-Br-GTP have high free energy barriers between the *syn* and *anti* conformations. However, H-REMD simulations using a few different λ-values (3 for GTP and 6 for 8-Br-GTP) suffice to enhance the conformational sampling enormously. The preference of *syn* and *anti* should follow quantitatively from the ensemble generated at the lowest λ-value corresponding to the unperturbed Hamiltonian of the REMD scheme. We compare the relative population of the two states with direct free energy calculations between them using hidden restraints along the glycosidic dihedral angle.

II. METHODS

The Methods section is divided into four parts. Firstly we discuss the implementation of soft-core interactions in REMD simulations. Secondly, we discuss the REMD simulations in more detail, and thirdly the use of hidden restraints to calculate the free energy difference between *syn* and *anti*. The section is concluded with a description of the exact simulation settings.

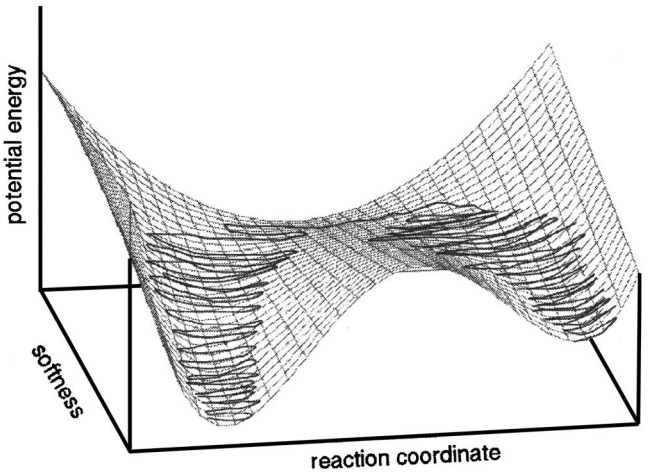

FIG. 2. Schematic representation of the energy profile as function of the softness of nonbonded interactions. Replicas at higher levels of softness convert more easily from one stable conformation to the other, which are separated by a high energy barrier if no softness is applied.

A. Implementation of soft-core interactions

We have used the following functional form for van der Waals and electrostatic soft-core interactions[7] between atoms i and j as a function of the interatomic distance r_{ij}

$$E_{ij}^{vdW}(r_{ij},\lambda) = \left(\frac{C12_{ij}}{A_{ij}(\lambda) + r_{ij}^6} - C6_{ij} \right) \frac{1}{A_{ij}(\lambda) + r_{ij}^6}, \quad (1)$$

$$E_{ij}^{el}(r_{ij},\lambda) = \frac{q_i q_j}{4\pi\varepsilon} \frac{1}{\sqrt{B_{ij}(\lambda) + r_{ij}^2}}, \quad (2)$$

with $A_{ij}(\lambda) = \alpha_{vdW}(C12_{ij}/C6_{ij})\lambda^2$ and $B_{ij}(\lambda) = \alpha_{el}\lambda^2$. $C12_{ij}$, $C6_{ij}$ are the Lennard–Jones parameters for atom pair i and j, q_i and q_j the partial charges of particles i and j, and α_{vdW} and α_{el} are the softness parameters. In the current study we used in all simulations $\alpha_{vdW} = \alpha_{el} = 1$, and the softness of the interactions was controlled through the parameter λ. It can be seen that at longer distances $[r_{ij} \gg A(\lambda)$ and $r_{ij} \gg B(\lambda)]$ the soft-core interaction approximates the interaction for normal atoms and that they differ mostly at short distances between the atoms $[r_{ij} \leqslant A(\lambda)$ or $r_{ij} \leqslant B(\lambda)]$. Potential energy barriers are mostly the result of a short-ranged repulsion between atoms, which can strongly be reduced by increasing the levels of softness. An idealized potential energy landscape for two states separated by a high barrier when no softness is applied, but part of the same energy valley at higher levels of softness is sketched in Fig. 2.

In GROMOS96 (Ref. 13) as well as GROMOS05 (Ref. 14) one can use soft-core interactions in the context of a free energy perturbation in which the interaction energy E_{ij} is written as a linear combination of the potential energy for two different states A and B,

$$E_{ij}(r_{ij},\lambda) = [1-\lambda]^n E^A(r_{ij},\lambda) + \lambda^n E^B(r_{ij},1-\lambda). \quad (3)$$

In cases where the Lennard–Jones parameters and partial charges are identical in states A and B and we set $\lambda = 0.5$ and $n = 1$, this reduces to the functional forms of Eqs. (1) and (2). For other λ-values one gets a mixture of potentials at different levels of softness. In order to be able to control the level

of softness by λ, which is convenient in a REMD setting, we extended the implementation of free energy perturbations in GROMOS05 to include the possibility to set individual λ-values for Lennard–Jones interaction (λ_{vdW}), the Lennard–Jones softness level λ_{soft}^{vdW}, Coulombic interactions (λ_{el}), and the Coulombic softness level (λ_{soft}^{el}) as a polynomial function (up to fourth order) of an overall or "global" λ-value. For the Lennard–Jones interaction we write the interaction energy as

$$E_{ij}^{vdW}(r_{ij},\lambda) = [1-\lambda_{vdW}(\lambda)]^n E_{ij}^{vdW,A}(r_{ij},\lambda_{soft}^{vdW}(\lambda)) + [\lambda_{vdW}(\lambda)]^n E_{ij}^{vdW,B}(r_{ij},1-\lambda_{soft}^{vdW}(\lambda)). \quad (4)$$

An analogous form can be written for the Coulombic interaction E_{ij}^{el}. For the REMD simulations of GTP and 8-Br-GTP reported here, we used individual λ-dependencies as follows:

$$\lambda_{vdW}(\lambda)=0, \quad \lambda_{soft}^{vdW}(\lambda)=\lambda, \quad (5)$$

$$\lambda_{el}(\lambda)=0, \quad \lambda_{soft}^{el}(\lambda)=\lambda. \quad (6)$$

With these settings the softness at individual replicas is easily controlled by the global lambda λ, while the actual interactions are only defined by the parameters defined for state *A*.

B. REMD

A REMD simulation involves *M* noninteracting copies (replicas) of MD of one system running in parallel at various conditions.[15] Let us mark the state of a REMD ensemble of simulations as $X=\{\ldots,x_m^i,\ldots,x_n^j,\ldots\}$, where the indices indicate that the *i*th replica is simulated at the *m*th condition and the *j*th replica is simulated at the *n*th condition. *x* represents the collected positions *q* and momenta *p* of all particles ($x\equiv(q,p)$). The weight factor for this state of the REMD ensemble is given by the product of Boltzmann factors for individual noninteracting replicas,

$$W_{REMD}(X)=\prod_{k=1}^{M} e^{-\beta_{m(k)}H_{m(k)}(q^k,p^k)}, \quad (7)$$

where $\beta_{m(k)}=1/k_BT_{m(k)}$ and $H_{m(k)}(q^k,p^k)$ is the Hamiltonian of the system given by sum of the kinetic energy $K(p)$ and the potential energy $E(q)$. k_B is the Boltzmann constant. The subscript $m(k)$ indicates the condition *m* at which replica *k* is currently simulated. In T-REMD, conditions *m* differ only by the temperature *T*, while in H-REMD, the condition represents different Hamiltonians, in this case described by the softness parameter λ. Conditions (λ or *T*) do not have to be different for all replicas. In a degenerate λ_{max}/T_{max} scheme,[11] multiple replicas are simulated at the same λ_{max}/T_{max} simultaneously, i.e., $m(i)=m(j)$.

At regular time intervals we attempt to exchange (switch) the conditions at which replicas i,j are simulated,

$$X=\{\ldots,x_m^i,\ldots,x_n^j,\ldots\}\rightarrow X'=\{\ldots,x_m^j,\ldots,x_n^i,\ldots\}. \quad (8)$$

In order to maintain the proper weight of the REMD ensemble as described in Eq. (7) a detailed balance condition must be imposed on the exchange probability,

$$w(X\rightarrow X')=\min[1,\exp(-\Delta)], \quad (9)$$

where

$$\Delta=\beta_m[H_m(q^j,p^j)-H_m(q^i,p^i)] - \beta_n[H_n(q^j,p^j)-H_n(q^i,p^i)]. \quad (10)$$

Sugita and Okamoto showed that the kinetic energy parts of the Hamiltonians cancel,[16] leading to

$$\Delta=\beta_m[E_{\lambda_m}(q^j)-E_{\lambda_m}(q^i)]-\beta_n[E_{\lambda_n}(q^j)-E_{\lambda_n}(q^i)]. \quad (11)$$

In the case of H-REMD, where all replicas are run at the same temperature, Δ reduces further to

$$\Delta=\beta[E_{\lambda_m}(q^j)-E_{\lambda_m}(q^i)-E_{\lambda_n}(q^j)+E_{\lambda_n}(q^i)]. \quad (12)$$

In our study the Hamiltonian applied for individual replicas is varied by introducing the soft-core interactions (1-2) controlled by parameter λ.

C. Thermodynamic integration using hidden dihedral angle restraints

The use of hidden dihedral angle restraints[17] offers an alternative approach to calculate the free energy difference between the *anti* and *syn* conformations of GTP/8-Br-GTP. A hidden dihedral angle restraint around the glycosidic bond was used to propagate the GTP/8-Br-GTP systems from one stable conformation to the other, thereby overcoming the energy barrier and sampling conformations on the transition path in an efficient way. The restraining energies for the dihedral angle ϕ(C4-N9-C1′-O4′) were calculated as a function of the coupling parameter λ according to Ref. 16,

$$V^{dihres}(\phi,\lambda)=4\lambda(1-\lambda)V_{restr}^{dihres,AB}(\phi,\lambda), \quad (13)$$

where

$$V_{restr}^{dihres,AB}(\phi,\lambda)=\begin{cases} V_{harm}^{dihres,AB}(\phi,\lambda) & \text{if } |\Delta\phi_\lambda|\leqslant\phi_{lin}^0 \\ V_{lin}^{dihres,AB}(\phi,\lambda) & \text{if } |\Delta\phi_\lambda|>\phi_{lin}^0, \end{cases} \quad (14)$$

with

$$\Delta\phi_\lambda=\phi-(1-\lambda)\phi_{0,A}-\lambda\phi_{0,B}+2n\pi, \quad (15)$$

and

$$V_{harm}^{dihres,AB}(\phi,\lambda)=1/2[(1-\lambda)K^A+\lambda K^B](\Delta\phi_\lambda)^2, \quad (16)$$

$$V_{lin}^{dihres,AB}(\phi,\lambda)=[(1-\lambda)K^A+\lambda K^B](\zeta\Delta\phi_\lambda-1/2\phi_{lin}^0)\phi_{lin}^0, \quad (17)$$

with $\zeta=-1$ if $\Delta\phi_\lambda<-\phi_{lin}^0$ and $\zeta=1$ if $\Delta\phi_\lambda>-\phi_{lin}^0$ for the linearized part of the restraint. We have used $K^A=K^B=100$ kJ rad^{-2} and $\phi_{lin}^0=30°$. For both GTP and 8-Br-GTP, four thermodynamic integration calculations were done: From −120° (*anti*) to 60° (*syn*) and back ($\phi^{0,A}=-120°$, $\phi^{0,B}=60°$ or $\phi^{0,A}=60°$, $\phi^{0,B}=-120°$), from 60° (*syn*) to 240° (*anti*) and back ($\phi_k^{0,A}=60°$, $\phi_k^{0,B}=240°$ or $\phi_k^{0,A}=240°$, $\phi_k^{0,B}=60°$).

As can be seen from Eq. (13) the restraint energy reduces to zero at the beginning ($\lambda=\lambda_A=0$) and end ($\lambda=\lambda_B=1$) states. Therefore an unperturbed relative free energy

TABLE I. Optimal REMD setting for GTP and 8-Br-GTP.

Molecule	λ_{max}	n	$t^{total}_{\lambda_{max}}$ (ps)	Optimal λ-set
GTP	0.45	4	100	[0.0,0.25,0.45,0.45,0.45,0.45]
8-Br-GTP	0.7	7	100	[0.0,0.2,0.4,0.55,0.65,0.7,0.7,0.7,0.7,0.7,0.7,0.7]

ΔG_{BA} of state B with respect to state A can be calculated using the thermodynamic integration method,[18]

$$\Delta G_{BA} = \int_{\lambda_A}^{\lambda_B} \left\langle \frac{\partial H}{\partial \lambda} \right\rangle_{\lambda} d\lambda, \tag{18}$$

where H is the Hamiltonian of the system including the restraining potential energy term, $V^{dihres}(\phi,\lambda)$, and the angular brackets indicate an ensemble average obtained at λ. The integration was performed by calculating the ensemble average $\langle \partial H/\partial \lambda \rangle_{\lambda}$ at discrete λ points, corresponding to angular changes of 20° ($\Delta\lambda=0.111$). In regions where the curvature of $\langle \partial H/\partial \lambda \rangle$ was high, the step size was halved. The initial sampling time for each λ point was 1 ns (after 100 ps relaxation which started from the equilibrated conformation of the simulation at the previous λ value). For λ points in which the ensemble averages did not converge to the same value in forward and reverse thermodynamic integration calculations, the sampling time was extended to 6 ns.

D. MD and REMD settings

All MD and REMD simulations were conducted using the GROMOS05 simulation package running on a linux cluster.[14] All bonds were constrained, using the SHAKE algorithm[19] with a relative geometric accuracy of 10^{-4}, allowing for a time step of 2 fs used in the leapfrog integration scheme.[20] Periodic boundary conditions, with a truncated octahedral box (average volume of 59.6 nm^3), were applied. After a steepest descent minimization to remove bad contacts between molecules, initial velocities were randomly assigned from a Maxwell–Boltzmann distribution at 298 K, according to the atomic masses. The temperature was kept constant using weak coupling to a bath of 298 K with a relaxation time of 0.1 ps.[21] The solute molecules (GTP or 8-Br-GTP) and solvent (i.e., 1926 explicit SPC water molecules[22] and three Na^+ counterions) were independently coupled to the heat bath. The pressure was controlled using isotropic weak coupling to atmospheric pressure with a relaxation time of 0.5 ps.[21] Van der Waals and electrostatic interactions were calculated using a triple range cutoff scheme. Interactions within a short-range cutoff of 0.8 nm were calculated every time step from a pair list that was generated every five steps. At these time points, interactions between 0.8 and 1.4 nm were also calculated and kept constant between updates. A reaction-field contribution was added to the electrostatic interactions and forces to account for a homogeneous medium outside the long-range cutoff, using the relative permittivity of SPC water (61).[23] All interaction energies were calculated according to the GROMOS force field, parameter set 53A6.[24] Force field parameters used for GTP and 8-Br-GTP are listed in the supplementary material.[25] In the H-REMD simulations, all sugar-base interactions in GTP and 8-Br-GTP are treated using the soft-core interactions through Eqs. (1), (2), and (4).

REMD is implemented in GROMOS05 such that only switches between "neighboring" replicas are attempted. Replica exchanges are attempted every 2.5 ps (elementary period, t^{elem}). However, not all replica pairs are considered at the same time. After an odd number of elementary periods, exchanges between the $(2i+1)$th and the $(2(i+1))$th replicas are attempted (we call them replica exchanges of type I) and after an even number of t^{elem} exchanges between the $(2i)$th and the $(2i+1)$th replicas are attempted (exchanges of type II). This means that the effective time between two switches of the same type is twice the elementary switching period (2×2.5 ps=5 ps). During the initial 40 t^{elem} (100 ps) no replica exchanges were attempted in order to equilibrate the systems at the individual replicas. The conformations were written out every 2.5 ps, just before the replica exchange attempt. In order to see how effective REMD is in sampling the less stable conformations, we started all REMD runs from the most stable conformation, i.e., in the case of GTP from *anti* and in the case of 8-Br-GTP from *syn* conformations.

A novel concept of degenerate λ_{max} simulations was applied as presented in our previous study.[11] In this approach more replicas (n) are simulated at the highest λ-value, λ_{max}, simultaneously and the time between switching attempts between these replicas is set such that every replica at λ_{max} spends a time $t^{total}_{\lambda_{max}}$, during which the system can convert from one conformation to the other. Usually $t^{total}_{\lambda_{max}} \gg t^{elem}$ because the conversion probability rather shows a sigmoidal than a linear time dependence, and the middle of the sigmoidal curve corresponds to a significantly longer time than t^{elem}. The values of λ_{max} and n as well as the number of λ-values between 0 and λ_{max} and their exact values were refined by the fast mimicking approach in Ref. 11. This approach maximizes the number of global conformational transitions (N_{gct}) per CPU. We defined the number of global conformational transitions as the number of times the conformational state changes for each particular replica when monitored at the lowest λ-value (λ_0). At which particular λ-value the conformational transition occurs is irrelevant for this measure. For more details, see Ref. 11. The λ-values at which REMD simulations were performed; $t^{total}_{\lambda_{max}}$ and n are summarized in Table I.

III. RESULTS

A. Standard MD simulations

Theoretically, one can obtain the populations of *syn* and *anti* conformations for GTP/8-Br-GTP from sufficiently long MD simulations, during which many *anti*↔*syn* transitions occur. However, 25 ns of MD simulation of GTP and 8-Br-

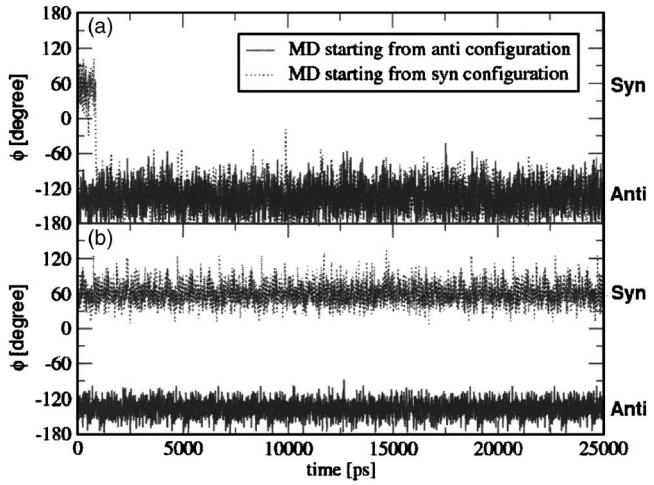

FIG. 3. Time dependence of dihedral angle (ϕ), around the glycosidic bond during two MD simulations (starting from *anti* and *syn* configurations) for (a) GTP and (b) 8-Br-GTP. *Anti* and *syn* conformational regions are indicated.

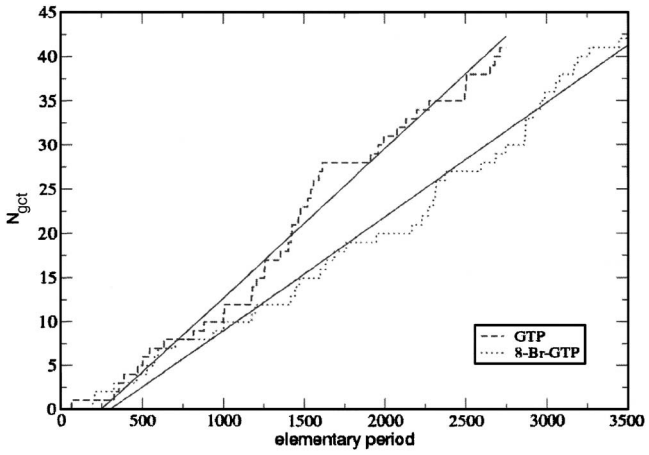

FIG. 4. Time dependence of the number of global transitions (N_{gct}) for REMD of GTP and 8-Br-GTP. Relaxation time calculated from the extrapolation of the linear part is for GTP 249 t^{elem} (elementary period, t^{elem} =2.5 ps) and for 8-Br-GTP 303 t^{elem}.

GTP shows that the *syn* and *anti* conformational states are separated by a quite high free energy barrier. For GTP we observe only one transition from the *syn* (less dominant) to the *anti* (more dominant) conformation and no transitions from *anti* to *syn* [Fig. 3(a)]. No transitions were observed at all for 8-Br-GTP, neither from *syn* to *anti* nor from *anti* to *syn* [Fig. 3(b)], indicating an even higher energy barrier between the *anti* and *syn* conformations for this molecule. This means that in order to obtain converged values of the *anti* and *syn* populations, we would have to run standard MD for an impractically long time. In such cases it may be very useful to use replica exchange MD, which can sample conformational space much more efficiently than standard MD.

B. REMD of GTP and 8-Br-GTP

All replicas within REMD were started from the same conformation (*anti* for GTP and *syn* for 8-Br-GTP). Therefore it takes some time to relax the complete set of REMD simulations. It is not straightforward to determine the relaxation time and time length of REMD simulation required to obtain sufficient statistics of measured quantities *a priori*. The REMD settings used here were chosen to maximize the number of global conformational transitions (N_{gct}) per CPU by fast mimicking.[11] Monitoring of N_{gct} is also useful for real REMD because when all replicas are in equilibrium, N_{gct} should show a linear time dependence. This allows us to determine the relaxation time of REMD by extrapolating the linear part of $N_{gct}(t)$ to 0 transition, as well as to estimate the length of REMD, which is needed to obtain a specific value of N_{gct}.

The time evolution of N_{gct} for GTP and 8-Br-GTP is shown in Fig. 4 from which the relaxation times are estimated to be 249 t^{elem} (622.5 ps) for GTP and 303 t^{elem} (757.5 ps) for 8-Br-GTP. This figure also shows that in order to reach at least 40 global conformational transitions, we perform REMD of GTP for 2750 t^{elem} (6875 ps) and REMD of 8-Br-GTP for 3500t^{elem} (8750 ps). Only the parts of the simulations after the relaxation times were used for quantitative analysis of these simulations.

The dihedral angle distributions of the glycosidic bond of GTP and 8-Br-GTP at different λ-values are shown in Figs. 5 and 6. The populations of *syn* and *anti* conformations obtained by integration of the distributions between bounds indicated in these figures are summarized in Tables II (GTP) and III (8-Br-GTP) together with the corresponding free energy difference between the *syn* and *anti* states as calculated by

$$\Delta G_{\text{syn-anti}} = -k_B T \ln \frac{[syn]}{[anti]}, \tag{19}$$

where k_B is again the Boltzmann constant and T=298 K. Usually we are most interested for values for unperturbed interactions (λ=0.0) which are for GTP,

$$[anti] = 95.6\ \% \ \pm 0.5\ \%\ ,$$

$$[syn] = 4.4\ \% \ \pm 0.5\ \%\ ,$$

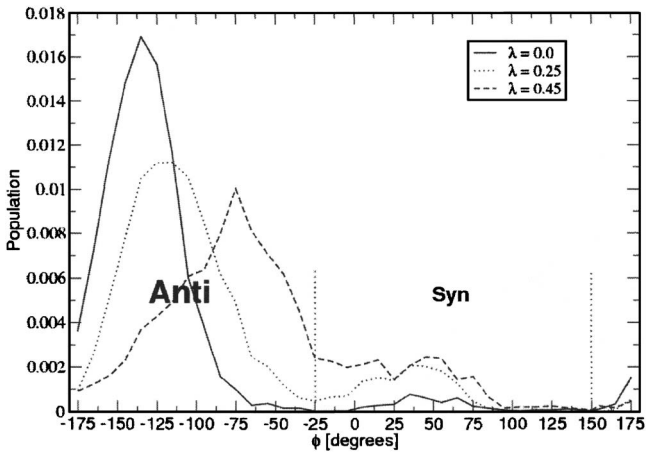

FIG. 5. Distribution of dihedral angle around the glycosidic bond of GTP at different levels of softness (λ). Populations were calculated using a bin width of 10°. *Anti* and *syn* conformational regions are indicated.

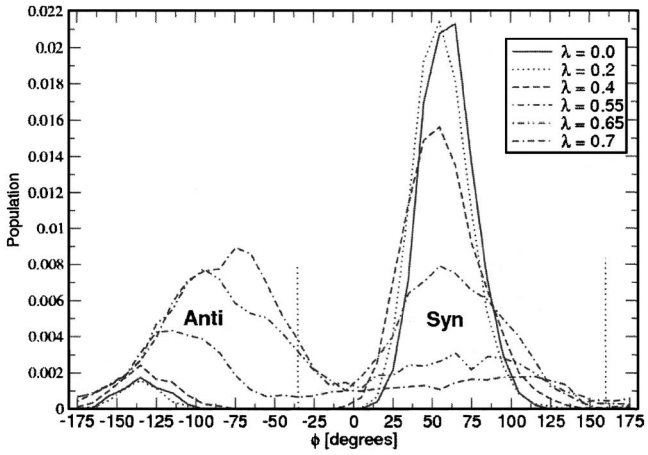

FIG. 6. Distribution of the dihedral angle around the glycosidic bond of 8-Br-GTP at different levels of softness (λ). Populations were calculated using a bin width of 10°. *Anti* and *syn* conformational regions are indicated.

$$\Delta G^{\mathrm{GTP}}_{\text{syn-anti}} = 7.6 \pm 0.3 \text{ kJ mol}^{-1},$$

and for 8-Br-GTP,

$$[anti] = 6.0\,\% \pm 1.8\,\%,$$

$$[syn] = 94.0\,\% \pm 1.8\,\%,$$

$$\Delta G^{\text{8-Br-GTP}}_{\text{syn-anti}} = -6.8 \pm 0.9 \text{ kJ mol}^{-1}.$$

Error estimates on the populations are calculated from block averages of occurrences of the conformational states followed by an extrapolation to infinite block length.[26]

C. Thermodynamic integration using a hidden dihedral angle restraint

The free energy difference between the *syn* and *anti* conformations can also be calculated by thermodynamic integration using a (hidden) dihedral angle restraint around the glycosidic bond. Theoretically, the obtained value for the free energy difference should not depend on the pathway by which the system is pulled from one stable conformation to another. However, in practice, this class of methods very often shows hysteresis resulting from inadequate relaxation of the systems at individual λ-values. In order to obtain reliable values, the free energy difference for both GTP and 8-Br-GTP was calculated through two different pathways $[-120°(anti) \leftrightarrow 60°(syn), 60°(syn) \leftrightarrow 240°(anti)]$ in both the forward and reverse directions (Figs. 7 and 8). This allows us to determine the convergence of the free energy difference and to monitor if sampling is sufficient for each point at the individual pathways. We note that similar values

TABLE II. Relative *syn* and *anti* conformational populations of GTP at different softness levels (λ). The corresponding free energy differences are also calculated.

λ	[*anti*]	[*syn*]	$\Delta G_{\text{syn-anti}}$(kJ mol^{-1})
0.0	0.954	0.044	7.62
0.25	0.860	0.140	4.49
0.45	0.768	0.232	2.96

TABLE III. Relative *syn* and *anti* conformational populations of 8-Br-GTP at different softness levels (λ). The corresponding free energy differences are also calculated.

λ	[*anti*]	[*syn*]	$\Delta G_{\text{syn-anti}}$(kJ mol^{-1})
0.0	0.060	0.940	−6.81
0.2	0.051	0.949	−7.24
0.4	0.187	0.813	−3.64
0.55	0.320	0.680	−1.67
0.65	0.619	0.381	1.20
0.7	0.722	0.278	2.36

of ΔG calculated from two opposite directions do not automatically mean a complete convergence. Figure 7(b) shows, for example, that although the calculated values of ΔG are very similar (-9.2 ± 1.2 and -9.5 ± 1.3 kJ/mol) there are still four λ-values (0.333; 0.5; 0.556; 0.667) at which the values of $\langle \partial H/\partial \lambda \rangle_\lambda$ differ more than the statistical error estimate. The conformational sampling for these points was not converged even after 6 ns, and the small hysteresis is obtained as the result of a fortuitous cancellation of errors. Note that two simulations that are sampling conformations belonging to different narrow minima can easily result in averages that do not converge to the same value, while both show small statistical error estimates. Indeed, we observed for λ-values right before and after the very local and steep conformational barriers that the harmonic dihedral angle restraint results in a dihedral angle distribution with two distinct maxima, sometimes with insufficient transitions between them to obtain converged results. Moreover, the true maximum of the barrier is in these cases still not sampled. From the four transition pathways shown in Figs. 7 and 8, only the $-120°(anti) \leftrightarrow 60°(syn)$ pathway for GTP shows a small

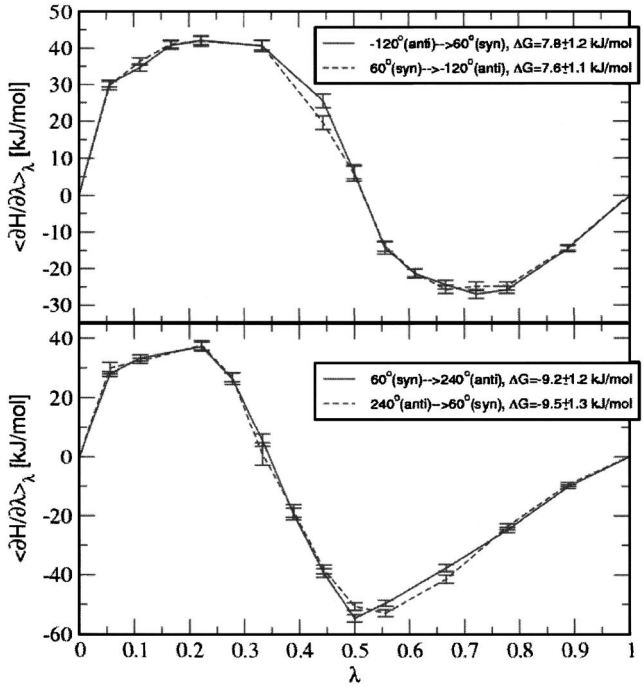

FIG. 7. Thermodynamic integration using hidden dihedral angle restraints for GTP. Error estimates for individual points result from block averaging and extrapolating the block length to infinity (Ref. 26).

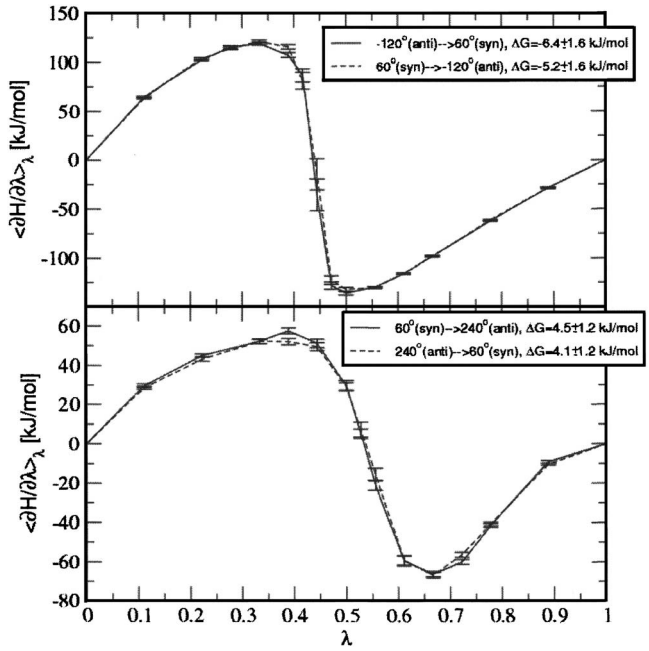

FIG. 8. Thermodynamic integration using hidden dihedral angle restraints for 8-Br-GTP. Error estimates for individual points result from block averaging and extrapolating the block length to infinity (Ref. 26).

hysteresis and the best convergence of $\langle \partial H/\partial \lambda \rangle_\lambda$ values in all λ-values. The steepness and curvature along this pathway also seems smallest. It leads to $\Delta G^{\mathrm{GTP}}_{\text{syn-anti}} = 7.7 \pm 1.2$ kJ mol^{-1} which is very similar to the value obtained from the REMD simulations of GTP ($\Delta G^{\mathrm{GTP}}_{\text{syn-anti}} = 7.6 \pm 0.3$ kJ mol^{-1}). Despite of the lack of full convergence in the other pathways, the calculated free energy differences for GTP ($\Delta G^{\mathrm{GTP}}_{\text{syn-anti}}$ between 9.2 and 9.5 ± 1.3 kJ/mol) and for 8-Br-GTP ($\Delta G^{\text{8-Br-GTP}}_{\text{syn-anti}}$ between −6.4 and -4.1 ± 1.6 kJ/mol) are still within k_BT (2.5 kJ mol^{-1}) from the values obtained from REMD simulations ($\Delta G^{\mathrm{GTP}}_{\text{syn-anti}} = 7.6 \pm 0.3$ kJ mol^{-1}, $\Delta G^{\text{8-Br-GTP}}_{\text{syn-anti}} = -6.8 \pm 0.9$ kJ mol^{-1}).

IV. DISCUSSION

Any experimental observable that depends on the molecular structures (e.g., ^{3}J-coupling values) does not result from one single conformation but from an average over many (all) conformations that are present and over the experimental collection time. In order to compare such experimental values with values obtained from calculation, it is essential to generate the proper ensemble of conformations corresponding to the same boundary conditions (temperature, pressure) as at which the experiment was performed. According to the ergodic theory, such an ensemble of conformations can be generated by sufficiently long MD simulations. However, in many biological systems the energy barriers separating different conformations are so high that MD of even hundreds of nanoseconds does not produce converged conformational ensembles.

Examples of such biological systems are GTP and its eight-substituted analog 8-Br-GTP which both have a high energy barrier between their *syn* and *anti* conformations. This barrier results from nonbonded interactions only. The dihedral angle term around the glycosidic bond for these molecules is zero in our models (see the force field parameters in the supplementary material).[25] While *anti* is the more dominant conformation for GTP, *syn* is the more dominant conformation for 8-Br-GTP. Experiments indicate, however, that the less dominant conformations are still present for non-negligible amounts of time (estimates range between 5% and 30%).[12,27] The presented study shows for both systems that two 25 ns MD simulations (one started from *anti* and one from *syn*) do not show any transition from the more to the less stable conformation.

One possible way to sample such rare events in a more efficient way is to force the system to cross the conformational barrier. The application of hidden restraints[17] belongs to this class of methods and was shown to converge faster to the free energy difference between unrestrained, stable, conformations than, e.g., umbrella sampling.[28] We applied a hidden dihedral angle restraint around the glycosidic bond to force transitions between the *anti* and *syn* conformations. This approach does not directly yield the proper ensemble of conformations, but such an ensemble can be approximated by generating separate ensembles around two conformational minima (*anti*, *syn*) and subsequently weight these ensembles according to the free energy difference between them. Despite its efficiency this method still required a relatively large number of simulations (14–16) and many of these simulations needed to be sampled for 6 ns in order to obtain a reasonable convergence. The total simulation time for GTP was 78 ns per pathway and for 8-Br-GTP 84 ns per pathway. Note that in this approach, the actual end-points of unrestrained *anti* or *syn* conformations are not simulated, but the free energy derivative is approximated as zero. These would still need to be simulated in order to approximate the conformational ensemble as indicated above. In reality, these states suffer from an end-state problem in which the derivative fluctuates with unrestrained motion. Extrapolations towards $\lambda = 0$ and $\lambda = 1$ show that zero is a better approximation. As is explained in Sec. III C, the full convergence for individual $\langle \partial H/\partial \lambda \rangle_\lambda$ values was obtained only for GTP along the $-120\,^\circ\,(anti) \leftrightarrow 60\,^\circ\,(syn)$ pathway and the calculated value of $\Delta G^{\mathrm{GTP}}_{\text{syn-anti}} = 7.7 \pm 1.2$ kJ mol^{-1} is in excellent agreement with $\Delta G^{\mathrm{GTP}}_{\text{syn-anti}} = 7.6 \pm 0.3$ kJ mol^{-1} obtained from REMD of GTP. The $\langle \partial H/\partial \lambda \rangle_\lambda$ values are reasonably (but not fully) converged for the other three pathways shown in Figs. 7 and 8, and the calculated $\Delta G^{\mathrm{GTP}}_{\text{syn-anti}}$ values are still within an acceptable range of 2.5 kJ mol^{-1} corresponding to thermal fluctuations when compared to values calculated from REMD.

The observed problems with the convergence of these simulations show that approaches which force the system to cross steep and high energy barriers are not necessarily computationally very efficient. Another important drawback of these methods is the requirement of a suitable reaction coordinate along which the system is forced to cross the energy barrier. This means that they can only be practically applied for simpler transition pathways.

REMD does not require prior knowledge about the transition path and can therefore be applied to more complex systems as well. In addition, REMD directly produces the proper ensemble of conformations. However, its efficiency can be much lower compared to methods forcing the mol-

ecule to cross a conformational barrier. As is explained in the Introduction, especially T-REMD becomes very inefficient for systems containing explicit solvent.[29] H-REMD involving a judiciously chosen perturbation of the Hamiltonian is less dependent on the overall system size and thus more generally applicable. On the other hand, it may not always be trivial to determine which parts of the Hamiltonian should be perturbed.

In the presented H-REMD scheme the Hamiltonian is modified over replicas by applying soft-core potentials for selected interactions. The efficiency is increased compared to other H-REMD approaches because soft-core potentials are very similar to unperturbed ones at longer distances. This means that only interactions between atoms that are close in distance (contributing most to the high energy barriers) contribute to the energy differences [Δ in Eq. (12)]. The switching probabilities are thus mainly governed by the interactions that really matter for enhancing the transitions over energy barriers. This is one of the main differences from other H-REMD schemes[5,6] or, e.g., the replica exchange with solute tempering[30] in which parts of the Hamiltonians are generally scaled rather than modified in their functional form (e.g., softened). For GTP and 8-Br-GTP only three (GTP) and six (8-Br-GTP) different levels of softness were required, thereby significantly reducing the time needed for the replicas to diffuse from the highest level of softness to the unperturbed Hamiltonian. In our previous study we showed that the overall efficiency can still be increased by simulating multiple replicas at the highest level of softness.[11] This leads to a total of six replicas for GTP and 12 replicas for 8-Br-GTP (Table I). The REMD simulations were performed such that after an initial equilibration period at least 40 global conformational transitions are observed. Both the equilibration time as well as the overall simulation time were obtained by monitoring the linear increase of the number of global transitions (N_{gct}). The total lengths of REMD simulation can then be calculated as $6\times 6.8=40.8$ ns for GTP and $12\times 8.7=104.4$ ns of 8-Br-GTP. When comparing these numbers with other methods (normal MD or thermodynamic integration with hidden restraints), one should keep in mind that REMD yields accurate free energy differences *and* the ensemble of relevant conformations for these molecules, which can be used for subsequent analysis.

In order to compare the efficiency of the presented H-REMD with standard T-REMD, we performed T-REMD for GTP using $T_0=298$ K and $T_{max}=540$ K at which *anti*$\leftrightarrow$*syn* conversions are regularly observed. 50 replicas, separated by 4 K (in the range of 298–370 K), 5 K (370–450 K), and 6 K (450–540 K), were needed to obtain an average switching probability of 22.5%, close to the optimal of 20%.[31] This high number of replicas already implicates a low efficiency of T-REMD for GTP in explicit water. Indeed, T-REMD for 1 ns per replica, i.e., a total length of 50 ns (as compared to 40.8 ns used in H-REMD) did not reveal any global conformational transitions at all despite the occurrence of transitions at higher temperatures. The efficiency of T-REMD for 8-Br-GTP in explicit water can be expected to be even worse because MD up to 1500 K does not show regular *anti*$\leftrightarrow$*syn* conversions.

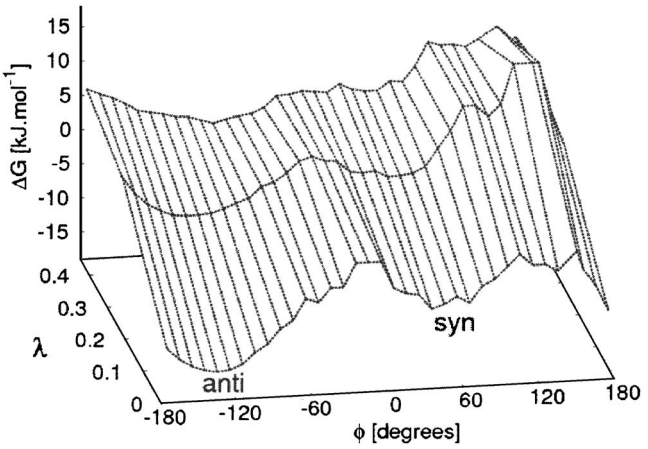

FIG. 9. Potential of mean force along the glycosidic bond of GTP as obtained from the populations in Fig. 5. Curves at individual λ-values were shifted in order to fulfill the perturbation formula (21) between different levels of softness for *anti* and *syn* conformations.

The dihedral angle distributions $P_\lambda(\varphi)$ in Figs. 5 and 6 allow us to generate the potential of mean force for GTP (Fig. 9) and for 8-Br-GTP (Fig. 10) using

$$G_\lambda(\varphi) = -k_B T \ln(P_\lambda(\varphi)) + C_\lambda, \tag{20}$$

where C_λ is a constant which is determined based on five φ points within the *anti* and *syn* regions such that the difference between $G_{\lambda j}(\varphi) - G_{\lambda i}(\varphi)$ is the same as calculated by the free energy perturbation formula,

$$\Delta G_{ij}(\varphi) = -k_B T \ln\langle e^{-(H_j - H_i)/k_B T}\rangle_i. \tag{21}$$

Figures 9 and 10 form the free energy landscapes on which the H-REMD simulations are performed and can be compared to the schematic representation in Fig. 2. Because of the nonmonotonous development of the free energy in the direction of λ for 8-Br-GTP, a three dimensional representation was very unclear. Rather, the individual curves are presented. The constant C_λ cancels exactly in the switching probability [Eqs. (9) and (12)] and is thus irrelevant for the REMD simulation. Figures 9 and 10 show that the soft-core

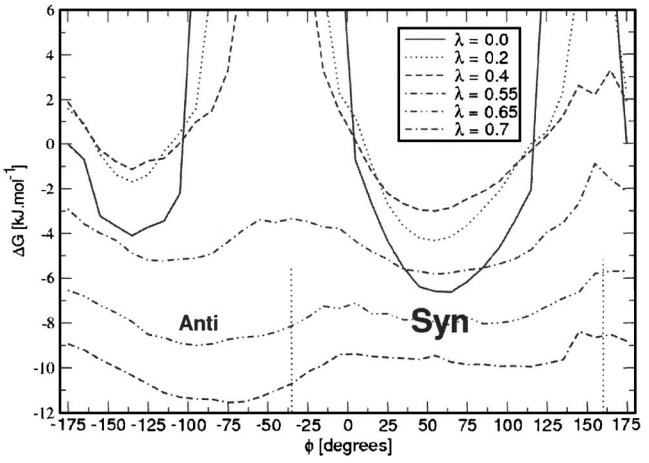

FIG. 10. Potential of mean force along the glycosidic bond of 8-Br-GTP as obtained from the populations in Fig. 6. Curves at individual λ-values were shifted in order to fulfill the perturbation formula (21) between different levels of softness for *anti* and *syn* conformations.

interactions at λ_{max} allow for a sufficient number of conformational transitions because (i) the conformational barrier is significantly decreased and (ii) the free energy difference between the stable conformations is reduced. This results in a higher population of the less dominant conformation and thus in a further increased occurrence of the conformational transitions. The free energy profiles also clearly show that the transitions between *anti* and *syn* conformations occur almost exclusively through the $-120°(anti) \leftrightarrow 60°(syn)$ pathway because the barrier for the $60°(syn) \leftrightarrow 240°(syn)$ pathway is significantly higher. Note that this is also the pathway in the thermodynamic integration simulations with hidden restraints that corresponds best to the REMD simulations. It is also interesting to observe how the interatomic interactions "lose" their local identity with increasing levels of softness. The nonsoft GTP and 8-Br-GTP have an inverse preference for the *syn* conformation (4.4% for GTP and 94% for 8-Br-GTP) but as can be seen from Tables II and III the *syn* populations become more similar with rising λ-values to a final 23.2% for GTP at $\lambda=0.45$ and 27.8% for 8-Br-GTP at $\lambda=0.7$. Furthermore, one may note that the position of the free energy minima is shifted at higher λ-values (most obvious for 8-Br-GTP at $\lambda=0.65$ and 0.7). This, of course, raises the question if the same dihedral angle intervals to define the *anti* and *syn* regions should be used for all λ-values and if the populations at these λ-values in Table III should not be revised. However, as these simulations involve unphysically perturbed molecules, the populations at these values have no direct meaning.

Even though GTP and 8-Br-GTP were used in this study mostly as model systems to show the application of our REMD simulations, there clearly is an interest in the conformational population of these molecules. Many six-or eight-substituted GTP and ATP analogs are being synthesized to act as specific inhibitors.[32–34] Bookser *et al.* correlated the binding affinities of such compounds to their *anti*/*syn* preference in water as obtained by ^{1}H NMR. Most adenosine analogs prefer the *syn* conformations, but the compounds with the highest adenosine kinase inhibitor potency all prefer the *anti* conformation. The methods described here may directly be applied to calculate the conformational preference prior to compound synthesis.

In the future, we think the H-REMD approach using soft-core interactions can be an asset to study (biomolecular) systems for which enhanced conformational sampling of a smaller part is required. Examples are loop regions of proteins (work in progress) or orientational sampling of small molecules bound to proteins (see, e.g., also our previous work involving binding free energy calculations using soft-core interactions[35,36]). The higher softness levels in these applications allow parts of the system to partially overlap and destabilize hydrogen bonds. Indeed, soft-core interactions allow us to see transitions which are not observed at high temperatures ($T=1000$ K) (unpublished results). This allows us to produce a wide variety of conformations of these parts of the system which are treated by soft-core interactions. Our approach may seem similar to two variants of T-REMD for local structure refinement: Partial and local replica exchange molecular dynamics.[37] These methods increase the temperature only in parts of the system. This will undoubtedly lead to a heat flow to the parts of the system that are still coupled to lower temperatures, but the assumption is made that this will not significantly modify the correct canonical ensemble. This is not guaranteed at all and can be different from system to system. Our approach does not induce a heat flow through the unperturbed system and does not require any such assumption. Moreover, it allows for even more flexibility by making it possible to select individual interactions (not only individual atoms or atom groups) which are treated by soft-core interactions, and each of these interaction can subsequently still respond to the same λ-value by specifying different values for α_{vdW} and α_{el} [Eqs. (1) and (2)].

As can be seen from the dihedral angle distributions in Figs. 5 and 6, the produced isothermic-isobaric ensemble does not only contain conformations from stable regions but also a few conformations from the energy barrier region. An approach involving only free energy estimates would not sample these conformations. We have calculated the populations of *syn* and *anti* conformations for GTP ($[anti]=0.956$, $[syn]=0.044$) and 8-Br-GTP ($[anti]$)$=0.060$, $[syn]=0.940$). These values compare qualitatively with NMR experiments for guanosine and 8-Br-guanosine in dimethylsulfoxide (DMSO).[12,27] We stress that these experiments involve a different molecule in a different solvent and that several assumptions underlay the estimates of populations from the original NMR data. However, from the experiments it is clear that 8-Br-GTP has an inverse population preference with respect to GTP. Calculations to compare to original NMR data are underway. For now, we would like to point out that the quality of the obtained populations does not only depend on the convergence of values due to the enhanced sampling (main aim of our study) but also on the accuracy of the force field parameters used for GTP and 8-Br-GTP. More relevant is therefore the quantitative comparison (discussed above) of the calculated free energy differences by the two described methods as these both used the same force field parameters.

V. CONCLUSIONS

We present a novel Hamiltonian REMD scheme using soft-core potentials, which allows for effective REMD simulations with only a few replicas. The application of the method was demonstrated for two realistic biomolecules, GTP and 8-Br-GTP, in explicit water. By using soft-core interactions we only perturb those parts of the Hamiltonian that contribute most to a local free energy barrier. This results in efficient H-REMD simulations using only a few different levels of softness (three for GTP and six for 8-Br-GTP) and thus to a fast diffusion of the replicas between the lowest and the highest levels of softness. In order to give the systems time to undergo conformational transitions at the highest level of softness, we applied a degenerate highest softness level scheme. The optimal settings of the H-REMD schemes were obtained from an optimization procedure as described in our previous study.[11] The optimization procedure utilizes the number of global conformational transitions. The time

dependence of this quantity was used to determine the relaxation and production times of H-REMD simulations. 40 global conformational transitions (20 from *anti* to *syn* and 20 from *syn* to *anti*) were observed within 6.8 ns of H-REMD simulation for GTP and 8.7 ns for 8-Br-GTP. No single transition from the more to the less dominant conformation was observed for either GTP or 8-Br-GTP within two 25 ns normal MD simulations (starting from initial *anti* and *syn* conformations) nor from T-REMD simulations of comparable length for GTP in explicit solvent. The obtained free energy differences between *anti* and *syn* conformations are in quantitative agreement with values calculated using thermodynamic integration with hidden dihedral angle restraints around the glycosidic bond and also in qualitative agreement with NMR estimates. The presented H-REMD approach using soft-core interactions allows for a softening of very specific, selected interactions which makes it a powerful technique to enhance the conformational sampling of smaller molecules in explicit solvent or of flexible parts of large biomacromolecules in explicit solvent.

ACKNOWLEDGMENTS

This work was supported by the Netherlands Genomics Initiative in the context of Horizon Breakthrough Grant No. 050-71-043 (J.H.) and by the Netherlands Organization for Scientific Research, VENI Grant No. 700.55.401 (C.O.).

[1] C. L. Brooks III, M. Karplus, and B. M. Pettitt, *Advances in Chemical Physics* (Wiley, New York, 1988), Vol. 71.
[2] M. Leitgeb, C. Schroder, and S. Boresch, J. Chem. Phys. **122**, 084109 (2005).
[3] J. P. Valleau and S. G. Whittington, in *Statistical Mechanics*, edited by B. J. Berne (Plenum, New York, 1977), Chap. 4, p. 145.
[4] U. H. E. Hansmann, Chem. Phys. Lett. **281**, 140 (1997).
[5] H. Fukunishi, O. Watanabe, and S. Takada, J. Chem. Phys. **116**, 9058 (2002).
[6] Y. Sugita, A. Kitao, and Y. Okamoto, J. Chem. Phys. **113**, 6042 (2000).
[7] T. C. Beutler, A. E. Mark, R. C. van Schaik, P. R. Gerber, and W. F. van Gunsteren, Chem. Phys. Lett. **222**, 529 (1994).
[8] D. D. Frantz, D. L. Freeman, and J. D. Doll, J. Chem. Phys. **93**, 2769 (1990).
[9] H. Li, G. Li, B. A. Berg, and W. Yang, J. Chem. Phys. **125**, 144902 (2006).
[10] A. Okur, D. R. Roe, C. Guanglei, V. Hornak, and C. Simmerling, J. Chem. Theory Comput. **3**, 557 (2007).
[11] J. Hritz and C. Oostenbrink, J. Chem. Phys. **127**, 204104 (2007).
[12] R. Stolarski, C. E. Hagberg, and D. Shugar, Eur. J. Biochem. **138**, 187 (1984).
[13] W. F. van Gunsteren, S. R. Billeter, A. A. Eising, P. H. Hünenberger, P. Krüger, A. E. Mark, W. R. P. Scott, and I. G. Tironi, *Biomolecular Simulation: The GROMOS96 Manual and User Guide* (Vdf Hochschulverlag AG an der ETH Zürich, Zürich, 1996).
[14] M. Christen, P. H. Hunenberger, D. Bakowies, R. Baron, R. Burgi, D. P. Geerke, T. N. Heinz, M. A. Kastenholz, V. Krautler, C. Oostenbrink, C. Peter, D. Trzesniak, and W. F. Van Gunsteren, J. Comput. Chem. **26**, 1719 (2005).
[15] R. H. Swendsen and J. S. Wang, Phys. Rev. Lett. **57**, 2607 (1986).
[16] Y. Sugita and Y. Okamoto, Chem. Phys. Lett. **314**, 141 (1999).
[17] M. Christen, A.-P. E. Kunz, and W. F. Van Gunsteren, J. Phys. Chem. B **110**, 8488 (2006).
[18] J. G. Kirkwood, J. Chem. Phys. **3**, 300 (1935).
[19] J.-P. Ryckaert, G. Ciccotti, and H. J. C. Berendsen, J. Comput. Phys. **23**, 327 (1977).
[20] R. W. Hockney, Methods Comput. Phys. **9**, 136 (1970).
[21] H. J. C. Berendsen, J. P. M. Postma, W. F. van Gunsteren, A. DiNola, and J. R. Haak, J. Chem. Phys. **81**, 3684 (1984).
[22] H. J. C. Berendsen, J. P. M. Postma, W. F. van Gunsteren, and J. Hermans, in *Intermolecular Forces*, edited by B. Pullman (Reidel, Dordrecht, 1981), p. 331.
[23] I. G. Tironi, R. Sperb, P. E. Smith, and W. F. van Gunsteren, J. Chem. Phys. **102**, 5451 (1995).
[24] C. Oostenbrink, A. Villa, A. E. Mark, and W. F. van Gunsteren, J. Comput. Chem. **25**, 1656 (2004).
[25] See EPAPS Document No. E-JCPSA6-128-509811 for force-field parameters of GTP and 8-Br-GTP. For more information on EPAPS, see http://www.aip.org/pubservs/epaps.html.
[26] M. P. Allen and D. J. Tildesley, *Computer Simulation of Liquids* (Clarendon, Oxford, 1987).
[27] H. Rosemeyer, G. Toth, B. Golankiewicz, Z. Kazimierczuk, W. Bourgeois, U. Kretschmer, H. P. Muth, and F. Seela, J. Org. Chem. **55**, 5784 (1990).
[28] G. M. Torrie and J. P. Valleau, J. Comput. Phys. **23**, 187 (1977).
[29] J. W. Pitera and W. C. Swope, Proc. Natl. Acad. Sci. U.S.A. **100**, 7587 (2003).
[30] P. Liu, B. Kim, R. A. Friesner, and B. J. Berne, Proc. Natl. Acad. Sci. U.S.A. **102**, 13749 (2005).
[31] A. Kone and D. A. Kofke, J. Chem. Phys. **122**, 206101 (2005).
[32] T. Läppchen, A. F. Hartog, V. A. Pinas, G. J. Koomen, and T. den Blaauwen, Biochemistry **44**, 7879 (2005).
[33] F. Schwede, A. Christensen, S. Liaw, T. Hippe, R. Kopperud, B. Jastorff, and S. O. Doskeland, Biochemistry **39**, 8803 (2000).
[34] B. C. Bookser, M. C. Matelich, K. Ollis, and B. G. Ugarkar, J. Med. Chem. **48**, 3389 (2005).
[35] B. C. Oostenbrink, J. W. Pitera, M. M. H. Van Lipzig, J. H. N. Meerman, and W. F. van Gunsteren, J. Med. Chem. **43**, 4594 (2000).
[36] C. Oostenbrink and W. F. van Gunsteren, Proteins **54**, 237 (2004).
[37] X. Cheng, G. Cui, V. Hornak, and C. Simmerling, J. Phys. Chem. B **109**, 8220 (2005).